presolar nebular environment (29). A more detailed study of the ISM abundance of Pb along the lines of Fig. 4 could help explore this interesting possibility further.

REFERENCES AND NOTES

1. A reported detection [M. Jura and W. H. Smith, *Astrophys. J.* **251**, L43 (1981)] of an optical line of Rb I ($Z = 37$), a trace ionization state in the ISM, was later shown to be incorrect (2). The original reported detection was attributed to a probable misidentification of a telluric feature.
2. S. R. Federman, C. Sneden, W. V. Schempp, W. H. Smith, *Astrophys. J.* **290**, L55 (1985).
3. E. Anders and N. Grevesse, *Geochim. Cosmochim. Acta* **53**, 197 (1989).
4. J. A. Cardelli, S. R. Federman, D. L. Lambert, C. E. Theodosiou, *Astrophys. J.* **416**, L41 (1993).
5. J. A. Cardelli, J. S. Mathis, D. C. Ebbets, B. D. Savage, *ibid.* **402**, L17 (1993).
6. J. A. Cardelli, U. J. Sofia, B. D. Savage, F. P. Keenan, P. L. Dufton, *ibid.* **420**, L29 (1994).
7. J. A. Cardelli, B. D. Savage, D. C. Ebbets, *ibid.* **383**, L23 (1991).
8. L. M. Hobbs, D. E. Welty, D. C. Morton, L. Spitzer, D. G. York, *ibid.* **411**, 750 (1993).
9. In the case of Pb, this corresponds to a sensitivity, relative to H_2, of 500 parts per trillion.
10. J. A. Cardelli and D. C. Ebbets, in *Attaining High Signal-to-Noise Data with the Goddard High Resolution Spectrograph* (Hubble Space Telescope Calibration Workshop, in press).
11. D. C. Morton, *Astrophys. J. Supp. Ser.* **77**, 119 (1991).
12. E. B. Jenkins, in *Interstellar Processes*, D. J. Hollenbach and H. A. Thronson, Eds. (Kluwer Academic, New York, 1987), pp. 533–559.
13. D. C. Morton, *Astrophys. J.* **197**, 85 (1975).
14. J. T. Wasson, *Meteorites: Their Record of the Early Solar System History* (Freeman, New York, 1985).
15. C. L. Joseph, *Astrophys. J.* **335**, 157 (1988).
16. S. R. Federman, Y. Sheffer, D. L. Lambert, R. L. Gilliland, *ibid.* **413**, L51 (1993).
17. B. D. Savage, J. A. Cardelli, U. J. Sofia, *ibid.* **401**, 706 (1992).
18. E. B. Jenkins, B. D. Savage, L. Spitzer, *ibid.* **301**, 355 (1986).
19. U. J. Sofia, J. A. Cardelli, B. D. Savage, *ibid.*, in press.
20. P. M. Griffen and J. W. Hutchenson, *J. Opt. Soc. Am.* **59**, 1607 (1969).
21. W. F. Chan, G. Cooper, X. Guo, G. R. Burton, C. E. Brion, *Phys. Rev. A* **46**, 149 (1992).
22. V. Trimble, *Astron. Astrophys. Rev.* **3**, 1 (1991).
23. C. J. Waddington, in *Origins of the Elements*, G. J. Mathews, Ed. (World, Singapore, 1988), p. 295.
24. M. J. Barlow, *Mon. Not. R. Astron. Soc.* **183**, 417 (1978).
25. This may also apply to some of the lighter elements. Observations of some young B-stars [D. R. Gies and D. L. Lambert, *Astrophys. J.* **387**, 673 (1992)] yield abundances of C and O that are below the solar values.
26. A. G. W. Cameron, *Astrophys. Space Sci.* **82**, 123 (1982).
27. C. M. Raiteri, R. Gallino, M. Busso, D. Neuberger, F. Kappler, *Astrophys. J.* **419**, 207 (1993).
28. R. Gallino, M. Busso, G. Picchio, C. M. Raiteri, in *Chemical and Dynamical Evolution of Galaxies*, F. Ferrini, J. Franco, F. Matteucci, Eds. (ETS Editrice, Pisa, 1990), p. 338.
29. U. Ott, *Nature* **364**, 25 (1993).

30. This research is based on observations obtained with the National Aeronautics and Space Administration (NASA)–European Space Agency Hubble Space Telescope through the Space Telescope Science Institute, which is operated by the Association of Universities for Research in Astronomy, Inc., under NASA contract NAS5-26555. I acknowledge useful discussions with D. L. Lambert, J. S. Mathis, and V. V. Smith. This research was supported under NASA's Long-Term Space Astrophysics Research Program (grant NAGW-2520).

3 March 1994; accepted 22 April 1994

On the Frequency-Locked Orbits of Two Particles in a Paul Trap

J. Hoffnagle* and R. G. Brewer

Calculations are presented that show frequency-locking to be a prominent phenomenon in the dynamics of two ions in a Paul trap, provided that damping is linear and small. The frequency-locked attractors that exist when dissipation is present correspond to stable, periodic orbits of the underlying Hamiltonian system, which appear to be infinite in number. The accuracy of the calculations is illustrated by comparing an orbit observed in a Paul trap for microspheres with the solution of the equations of motion.

Ion traps offer researchers the opportunity to study individual ions, which are nearly at rest and largely free from external perturbations, and these traps have important applications in spectroscopy, quantum optics, and metrology. When radiation pressure is used to cool trapped ions to millikelvin temperatures (1), unusual and interesting dynamical systems appear, Coulomb clusters, in which the electrostatic potential energy is large compared with the random thermal energy. The equations of motion of particles in a Paul trap are independent of the particle size, and several important dynamical phenomena, including transitions between ordered and chaotic motion, were first observed in an experiment on trapping of charged aluminium particles (2). But widespread interest in Coulomb cluster dynamics only followed the introduction of laser cooling and the observation in Paul traps of "ion crystals" (3, 4), for which the time-averaged confining force is just balanced by the ions' mutual electrostatic repulsion, yielding regular arrays in which the ions oscillate with the trap frequency about their average positions.

Most work on trapped ion dynamics has focused on crystals, chaos, and the transition between these two states of motion (5–7). In particular, a transition from transient to stationary chaos was found when the trap parameters were varied (8). The crystal is not, however, the only regular solution of the equations of motion: in this report we show that frequency-locking (5, 9) is a prevalent feature of trapped ion dynamics and that, in general, the two-ion system is multistable, with many coexisting frequency-locked attractors. Although periodic orbits of two ions in a Paul trap were predicted several years ago, they were largely neglected, because only the crystal was observed in trapped ion experiments. We present the results of a systematic, numerical study of frequency-locking as the trap voltage and energy dissipation are varied. These results suggest that as the dissipation tends to zero, the number of frequency-locked orbits becomes infinite. It is notable that celestial mechanics, in which the nonlinear gravitational interaction has the same form as the electrostatic interaction between ions, is also rife with instances of frequency-locking (10); the orbital resonance by which Neptune and Pluto avoid close approaches, although their orbits cross, is particularly reminiscent of the ion trajectories.

We consider the simplest, nontrivial Coulomb cluster in a Paul trap—that of two ions. This is a particularly elementary problem in classical, nonlinear dynamics: two particles of charge e and mass m in a periodic electric potential

$$V(\mathbf{r},t) = (V_{DC} - V_{AC}\cos\Omega t)\frac{x^2 + y^2 - 2z^2}{2r_0^2} \quad (1)$$

where r_0 is a characteristic trap radius and V_{DC} and V_{AC} are the amplitudes of the applied potential with frequencies zero and Ω, respectively. The equations of motion separate into center-of-mass and relative components, the former obeying the same, linear Mathieu equation as does a single trapped particle. Therefore, we may restrict our attention to the relative coordinate $\mathbf{r}_{12}$, expressed in cylindrical coordinates as (r,ϕ,z). If dissipation is present, it damps the angular momentum L_ϕ, leaving two degrees of freedom. Introducing dimensionless units for time, $\tau = \Omega t/2$, and the electric potentials, $a = -8eV_{DC}/mr_0^2\Omega^2$, $q = 4eV_{AC}/mr_0^2\Omega^2$, and measuring length in units of $[\ell] = (2e^2/m\Omega^2)^{1/3}$, the equations of motion become coupled Mathieu-Coulomb equations:

IBM Almaden Research Center, 650 Harry Road, San Jose, CA 95120, USA.

*To whom correspondence should be addressed.

$$\ddot{r} + \Gamma\dot{r} + (-a/2 + q \cos 2\tau - r_{12}^{-3})r = 0$$
$$\ddot{z} + \Gamma\dot{z} + (a - 2q \cos 2\tau - r_{12}^{-3})z = 0 \tag{2}$$

Dots denote differentiation with respect to τ, and the term in Γ describes linear damping of the particle velocity.

Without the terms in r_{12}^{-3}, the equations of motion (Eqs. 2) would separate into independent Mathieu equations (*11*), the solutions to which can be visualized as a superposition of driven motion at the trap frequency (equal to 2 in our dimensionless units) and secular oscillations at frequencies $0 < \beta_r, \beta_z < 1$, which are transcendental functions of the parameters a and q. The Coulomb term couples the radial and axial motions in a nonlinear way and can perturbatively pull the free oscillation frequencies to rational values having a common denominator, resulting in frequency-locking. The ratios of the locked frequencies to the trap frequency are referred to as the winding numbers (*12*) w_r and w_z. For example, with $a = 0$ and $q = 0.6$, the Mathieu equation solutions have $\beta_r/2 = 0.1080$ and $\beta_z/2 = 0.2311$. A numerical solution of the Mathieu-Coulomb equations (Eqs. 2) predicts a frequency-locked orbit with $w_r = 1/10$ and $w_z = 2/10$ and, hence, a period 10 times that of the trap potential. The calculated trajectories are shown in Fig. 1A; one particle moves along the arc having $z > 0$ over most of its range, and the other moves along the arc with $z < 0$. Although the orbits cross, the particles do not collide; rather, they avoid each other, and the center of mass remains fixed at the origin.

Frequency-locking of trapped ions has not been reported, probably because the interaction of the ions with laser light, which is necessary for cooling and viewing the ions, is highly nonlinear in the velocity. Calculations indicate that this additional nonlinearity acts to destabilize the frequency-locked orbits. To circumvent this problem, we have constructed a Paul trap (*2*) for micrometer-sized, electrostatically charged polymer spheres (*13*). Note that the equations of motion (Eqs. 2) are the same for ions and microspheres, because they do not depend on the absolute charge and mass of the trapped particles, but only on dimensionless combinations of these quantities and the trap parameters. When the apparatus is evacuated to approximately 1 Pa, drag from the residual gas is linear in the velocity and corresponds to $\Gamma \sim 10^{-3}$ to 10^{-2}. A photograph of two microspheres in the Paul trap at $q = 0.6$ (Fig. 1B) shows excellent agreement with the calculated orbit. The motion is stable and has been observed to persist for hours but is very sensitive to disturbances such as vibrations of the apparatus. Sufficiently large perturbations typically result in the particles reverting to the crystal.

Experiments located four other frequency-locked orbits, stable over ranges of q that agreed well with the calculations (*13*). However, computations also indicated the existence of orbits that were stable over very small ranges of q, which were apparently too easily perturbed to be seen in our apparatus. To investigate the prevalence of frequency-locking in the idealized system (Eqs. 2), we performed a systematic search for stable, periodic solutions with $\Gamma = 10^{-3}$, $a = 0$, and $0.7 \leq q \leq 0.908$. This parameter range is of interest because there is a transition (*8*) from transient to stationary chaos near $q = 0.87$, slightly less than the value $q_M = 0.908046$ at which the center-of-mass motion becomes unbounded. For every value of q, in steps of 10^{-3}, 20 sets of random initial conditions were chosen, and the Mathieu-Coulomb equations (Eqs. 2) were numerically integrated with a Bulirsch-Stoer algorithm (*14*). After every cycle of the trapping potential, the four phase space coordinates were recorded, and after every 100 cycles, a comparison was made with the previous 100 sets of coordinates. If all coordinates of two points separated by P trap cycles coincided to within 2×10^{-3}, the orbit was considered a candidate for periodicity. Each trajectory was monitored for 5×10^5 trap periods or until a coincidence was found. Each candidate orbit was then examined in more detail with the interactive program "Dynamics" (*15*). The winding numbers were verified, and the range of q and Γ over which the orbit was stable was also established. In this way, 81 orbits with $P \leq 100$ were located, with winding numbers that generally approximate the corresponding frequency ratios of the linear Mathieu equations (Fig. 2). For a given value of q there are multiple coexisting, periodic attractors, and the ultimate fate of a given trajectory depends on the initial conditions. Note that the crystal, which is stable over the entire range $0 < q < q_M$, is also periodic and can be regarded as the simplest frequency-locked state, with $(w_r, w_z) = (1/1, 0/1)$.

The method for finding the periodic orbits takes advantage of dissipation, which causes trajectories to converge to attractors,

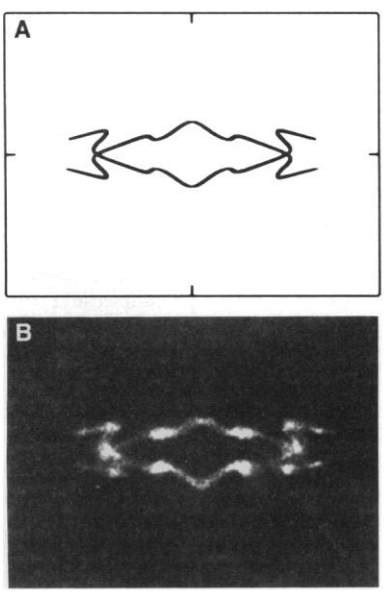

Fig. 1. Frequency-locked orbit with w_r:w_z:Ω = 1:2:10 at q = 0.6. (**A**) Computed trajectories. The horizontal (r) axis extends from −12 to +12 dimensionless units and the vertical (z) axis from −9 to +9. (**B**) Photograph of two microspheres in a Paul trap. The exposure was 1 s, corresponding to seven periods of the motion.

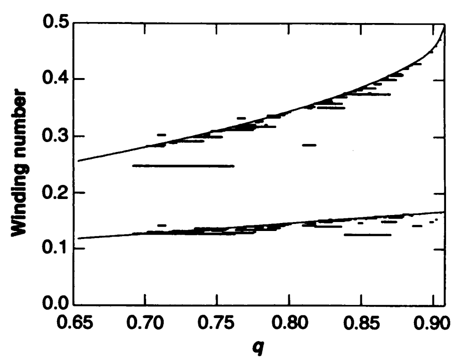

Fig. 2. Stable, periodic orbits for $\Gamma = 1 \times 10^{-3}$. Each orbit is represented by a pair of horizontal bars. Their vertical positions indicate w_r and w_z, and their horizontal extent indicates the range of stability in q. (In some cases where orbits with the same w_r but different w_z coexist for a given q, the bars representing w_r are slightly offset vertically to make them distinguishable.) The thin curves show the corresponding frequency ratios, $\beta_r/2$ and $\beta_z/2$, in the absence of the Coulomb term.

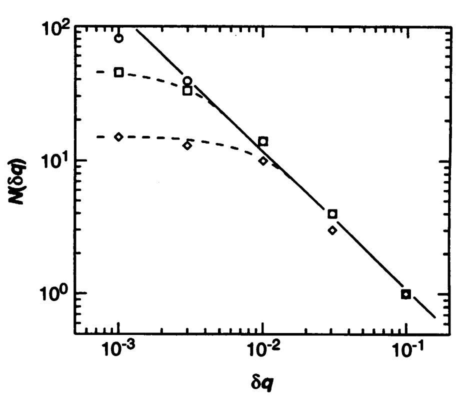

Fig. 3. Number of periodic orbits versus minimum stability range. Circles: $\Gamma = 1 \times 10^{-3}$; squares: $\Gamma = 3 \times 10^{-3}$; diamonds: $\Gamma = 1 \times 10^{-2}$. For large δq the points coincide. The solid line is a fit of the points with $\Gamma = 1 \times 10^{-3}$ and $\delta q \geq 3 \times 10^{-4}$ to a power-law dependence, yielding $\gamma = 1.02$, and the dashed lines connecting the points with the same values of Γ are to guide the eye.

but because Γ is small, it is not surprising that there is a close connection between the dynamics of the dissipative system and the Hamiltonian system obtained when $\Gamma = 0$. Every frequency-locked orbit evolves smoothly as $\Gamma \rightarrow 0$ to a stable, periodic orbit of the Hamiltonian system. In fact, increasing the damping destabilizes the periodic orbits; in each case there exists a maximum value of Γ above which the orbit becomes unstable. As a general rule, the orbits (Fig. 2) that become unstable at small values of Γ are those that extend over small ranges of q; they also tend to have large periods. We therefore consider $N(\delta q)$, the total number of periodic solutions that are stable over a range of greater than δq, as a function of δq, for three values of Γ (Fig. 3). One sees that the orbits with δq less than about $\Gamma/10$ are destroyed. A similar instance of the destruction of multistable, periodic orbits by dissipation has also been reported for a system of two coupled Van der Pol oscillators (*16*).

The scaling of $N(\delta q)$ with q (Fig. 3) suggests that in the limit $\Gamma \rightarrow 0$ there are an infinite number of periodic orbits, stable over small ranges of q according to a power law

$$N(\delta q) = \delta q^{-\gamma} \quad (3)$$

A similar power-law dependence is observed for one-dimensional circle maps at the critical value of the nonlinearity, in which case γ is the fractal dimension of the "devil's staircase" of frequency-locked states (*12*). Unfortunately, our computational resources do not allow us to locate enough periodic orbits to see whether their distribution in q is self-similar. The exponent γ can be extracted by linear regression of the points with $\Gamma = 1 \times 10^{-3}$. The value of N for $\delta q = 1 \times 10^{-4}$ is probably depressed by damping and because the search for periodic orbits was limited to periods no greater than 100 trap cycles. Excluding this point gives $\gamma = 1.02 \pm 0.05$ (correlation coefficient $r = 0.997$), distinctly different from the universal value of 0.87 seen in circle maps at criticality.

The well-known ion crystals seen in Paul traps are thus seen to be the most stable members of a much larger class of frequency-locked states. The underlying Hamiltonian dynamics exhibits an apparently infinite number of stable, periodic orbits with winding numbers that are rational approximants of the secular frequencies associated with the Mathieu functions for the same parameter values. With increasing dissipation, the complicated phase space structure of the Hamiltonian system becomes progressively simpler. For infinitesimal damping, the stable, periodic orbits correspond to frequency-locked attractors; then as the dissipation increases, the attractors are gradually destroyed until, for sufficiently large damping, only the crystal remains.

REFERENCES AND NOTES

1. W. Neuhauser, M. Hohenstatt, P. Toschek, H. Dehmelt, *Phys. Rev. Lett.* **41**, 233 (1978).
2. R. F. Wuerker, H. Shelton, R. V. Langmuir, *J. Appl. Phys.* **30**, 342 (1959).
3. F. Diedrich, E. Peik, J. M. Chen, W. Quint, H. Walther, *Phys. Rev. Lett.* **59**, 2931 (1987).
4. D. J. Wineland, J. C. Bergquist, W. M. Itano, J. J. Bollinger, C. H. Manney, *ibid.*, p. 2935.
5. J. Hoffnagle, R. G. DeVoe, L. Reyna, R. G. Brewer, *ibid.* **61**, 255 (1988).
6. R. Blümel *et al.*, *Nature* **334**, 309 (1988).
7. R. Blümel, C. Kappler, W. Quint, H. Walther, *Phys. Rev. A* **40**, 808 (1989).
8. R. G. Brewer, J. Hoffnagle, R. G. DeVoe, *Phys. Rev. Lett.* **65**, 2619 (1990).
9. ———, L. Reyna, W. Henshaw, *Nature* **344**, 305 (1990).
10. W. M. Kaula, *An Introduction to Planetary Physics* (Wiley, New York, 1968).
11. M. Abramowitz and I. A. Stegun, *Handbook of Mathematical Functions* (Government Printing Office, Washington, DC, 1968).
12. M. H. Jensen, P. Bak, T. Bohr, *Phys. Rev. A* **30**, 1960 (1984).
13. J. Hoffnagle and R. G. Brewer, *Phys. Rev. Lett.* **71**, 1828 (1993).
14. N. H. Press, B. P. Flannery, S. A. Teukolsky, W. T. Vetterling, *Numerical Recipes* (Cambridge Univ. Press, Cambridge, 1987).
15. J. A. Yorke, *Dynamics* (Univ. of Maryland, College Park, MD, 1990). Available from the author on request.
16. P. M. Battelino, C. Grebogi, E. Ott, J. A. Yorke, E. D. Yorke, *Physica D* **32**, 296 (1988).

1 March 1994; accepted 18 May 1994

Surface Pinning as a Determinant of the Bulk Flux-Line Lattice Structure in Copper Oxide Superconductors

Seokwon Yoon, Hongjie Dai, Jie Liu, Charles M. Lieber*

Direct knowledge of crystal defects and their perturbation of magnetic flux lines is essential to understanding pinning and to devising approaches that enhance critical currents in superconductors with high critical temperatures (T_c). Atomic force microscopy was used to simultaneously characterize crystal defects and the magnetic flux-line lattice in single crystals of $Bi_2Sr_2CaCu_2O_8$. Images show that surface defects, which are present on all real samples, pin the flux-line lattice. Above a critical height, the pinning interaction is sufficiently strong to form grain boundaries in the bulk flux-line lattice. These results elucidate the structure of the defects that pin flux lines and demonstrate that surface pinning, through the formation of grain boundaries, can determine the bulk flux-line lattice structure in high-T_c materials. The implications of these results to the bulk flux-line lattice structure observed in previous experiments and to enhancing critical currents are discussed.

Understanding the structure and pinning of the magnetic flux-line lattice (FLL) in the high-T_c copper oxide superconductors is a challenging problem of central importance to many applications proposed for these materials (*1*). Two techniques, neutron diffraction (*2–4*) and Bitter decoration (*5–9*), have been used to probe the structure of the FLL in the copper oxide materials. Neutron scattering experiments probe the FLL of the bulk material but, as in any diffraction experiment, cannot provide microscopic details of the FLL (for example, topological defects). Furthermore, neutron diffraction experiments have not provided direct information about crystalline defects that might pin the FLL. On the other hand, Bitter patterns, which are produced when individual flux lines are decorated with small magnetic particles as they emerge from the surface of a superconductor, can be used to address directly the microscopic structure of the FLL. This microscopic view has led to the identification of several structures, including a hexatic glass (*6*), a chain state (*7, 8*), and grain boundaries (*9*).

The conventional Bitter decoration technique is limited in several respects. It is implicitly assumed that the surface structure probed by this technique is representative of the bulk FLL. This assumption has been questioned theoretically (*10*) because the flux lines in the copper oxide materials have both a large line energy, which makes them susceptible to pinning by surface roughness, and a small line tension, which makes them flexible. Hence, flux lines pinned by surface defects could bend and adopt a different structure in the bulk. There is some experimental evidence from Bitter patterns for pinning of the FLL by surface roughness (*9*); however, it is still unclear whether the FLL seen at the surface is the same or differs from that of the bulk. This situation is not surprising because the techniques used to view the patterns, electron or optical microscopy, provide little quantitative infor-

Division of Applied Sciences and Department of Chemistry, Harvard University, Cambridge, MA 02138, USA.

*To whom correspondence should be addressed.